Recent Advances in Avalanche Photodiodes

Joe C. Campbell, *Fellow, IEEE*, Stephane Demiguel, Feng Ma, Ariane Beck, Xiangyi Guo, Shuling Wang, Xiaoguang Zheng, Xiaowei Li, Jeffrey D. Beck, *Senior Member, IEEE*, Michael A. Kinch, Andrew Huntington, Larry A. Coldren, *Fellow, IEEE*, Jean Decobert, and Nadine Tscherptner

Invited Paper

***Abstract*—The development of high-performance optical receivers has been a primary driving force for research on III-V compound avalanche photodiodes (APDs). The evolution of fiber optic systems toward higher bit rates has pushed APD performance toward higher bandwidths, lower noise, and higher gain-bandwidth products. Utilizing thin multiplication regions has reduced the excess noise. Further noise reduction has been demonstrated by incorporating new materials and impact ionization engineering with beneficially designed heterostructures. High gain-bandwidth products have been achieved waveguide structures. Recently, imaging and sensing applications have spurred interest in low noise APDs in the infrared and the UV as well as large area APDs and arrays. This paper reviews some of the recent progress in APD technology.**

***Index Terms*—Avalanche photodiodes (APDs), impact ionization, infrared, multiplication noise, photodetectors, ultraviolet (UV).**

I. Introduction

INITIAL development of III-V compound avalanche photodiodes (APDs) was driven by fiber optic telecommunications, primarily for high-bit-rate, long-haul receivers. Compared to receivers with p-i-n photodiodes, those that utilize APDs achieve 5–10 dB better sensitivity. For these devices, research focused on reducing the excess noise and developing structures with high gain-bandwidth products to accommodate the ever-increasing bit rates of fiber-optic systems. Recently, imaging applications such as three-dimensional (3-D) imaging, sensing, and space-related spectroscopy have stimulated interest in APD arrays and large area devices that operate in the UV and short wavelength infrared (SWIR) range $(0.8\ \mu\text{m} \leq \lambda \leq 2.2\ \mu\text{m})$. For these tasks, speed is not critical, but it is essential to attain very low dark current densities and low multiplication noise. In this paper, we will review some of the recent developments that have brought about improved APD performance.

Manuscript received March 4, 2004; revised June 4, 2004. This work was supported by the Defense Advanced Research Projects Agency through the Center for Chips with Heterogeneously Integrated Photonics, the 3-D Imaging Program, and the Semiconductor Ultraviolet Optical Sources (SUVOS) Program.

J. C. Campbell, S. Demiguel, F. Ma, A. Beck, X. Guo, S. Wang, X. Zheng, and X. Li are with the Microelectronics Research Center, The University of Texas at Austin, Austin, TX 78712 USA (e-mail: jcc@mail.utexas.edu).

J. D. Beck and M. A. Kinch are with DRS Infrared Technologies, LP, Dallas, TX 75374 USA.

A. Huntington and L. A. Coldren are with the Materials Department, Optoelectronics Technology Center, University of California at Santa Barbara, Santa Barbara, CA 93106 USA.

J. Decobert and N. Tscherptner are with Alcatel R&I, 91460 Marcoussis, France.

Digital Object Identifier 10.1109/JSTQE.2004.833971

II. Low-Noise APDs

The multiplication region of an APD plays a critical role in determining the gain, the multiplication noise, and the gain-bandwidth product. According to the local-field avalanche theory [1]–[3], both the multiplication noise and the gain-bandwidth product of APDs are determined by the electron, α, and hole, β, ionization coefficients of the material in the multiplication region; better performance is achieved when one of the ionization coefficients is much larger than the other, i.e., the β/α ratio (k) deviates markedly from unity. Since k is a material property, efforts to improve APD performance have focused on optimizing the electric field profile and characterizing new materials. For example, it has recently been reported that k $\sim$ 0.15 to 0.19 for $Al_xGa_{1-x}As$ $(x \geq 0.8)$. [4]–[6]

Some compositions of $Hg_{1-x}Cd_xTe$ appear to exhibit even lower k values. Beck *et al.* [7] have observed exponential gain curve and extremely low multiplication noise ($F(M) \sim 1$ for multiplication, M, up to 100) in $Hg_{0.7}Cd_{0.3}Te$ APDs. These phenomena suggest that k ~ 0. Unlike most III-V semiconductors, $Hg_{0.7}Cd_{0.3}Te$ has a very small band gap (0.29 eV) for the Γ valley, and very high L and X valleys (1.5 and 2.5 eV, respectively [8]). The band structure suggests that in a $Hg_{0.7}Cd_{0.3}Te$ APD, electrons have a very small intervalley phonon scattering rate, which is the dominant scattering mechanism in most III-V semiconductors. In addition, the large effective mass ratio $(m_h/m_e \sim 30)$ indicates that there is a large difference in the phonon and alloy scattering rates of holes and electrons for transport in $Hg_{0.7}Cd_{0.3}Te$. This picture is supported by the measured high electron mobility (two orders of magnitude higher than hole mobility) in HgCdTe materials. [9]

We have developed a Monte Carlo model to quantitatively study impact ionization in $Hg_{1-x}Cd_xTe$. For this study, the band structure of $Hg_{0.7}Cd_{0.3}Te$, including the Γ, L and X valleys of the conduction band, and heavy hole, light hole, and split-off valance bands, was incorporated into the model. Using a Keldysh formula [10] for impact ionizations, and threshold energies of 0.3 and 0.6 eV [11], respectively, for electrons and holes, the simulated gain and noise for an APD with a 3-μm-thick intrinsic region are shown as dashed lines in Fig. 1. This simulation assumes that electrons are injected from the

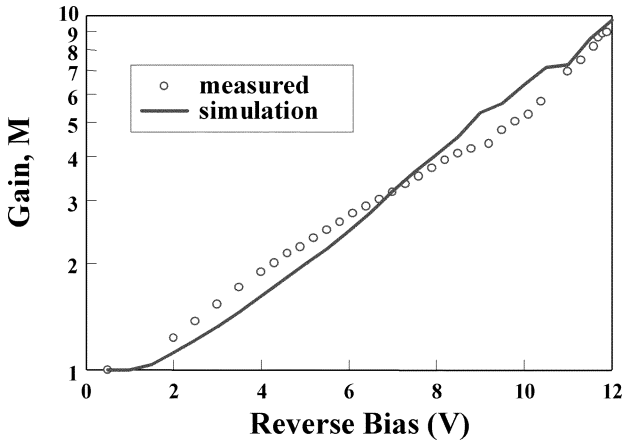

Fig. 1. Simulated (o) and measured (solid line) (a) gain and (b) excess noise factor of a 3-μm-thick cylindrical $Hg_{0.7}Cd_{0.3}Te$ APD.

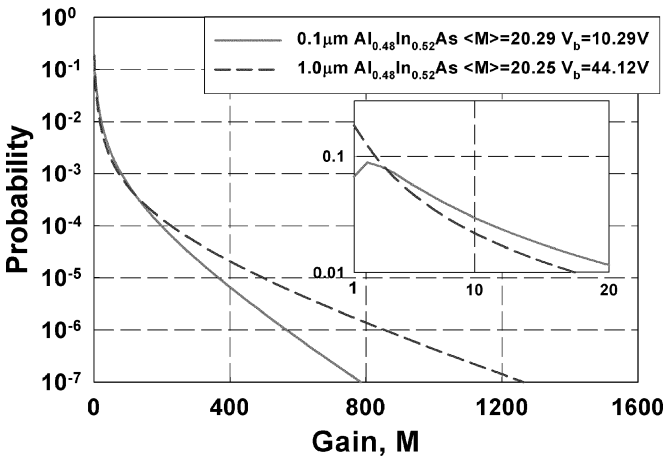

Fig. 2. Comparison of the gain distribution curves for $Al_{0.48}In_{0.52}As$ APDs having multiplication region widths of 1.0 (dashed line) and 0.1 μm (solid line). The average gain for both APDs is M $\sim$ 20 but the excess noise factors for the 1.0 and 0.1 μm APDs is 6.9 and 4, respectively.

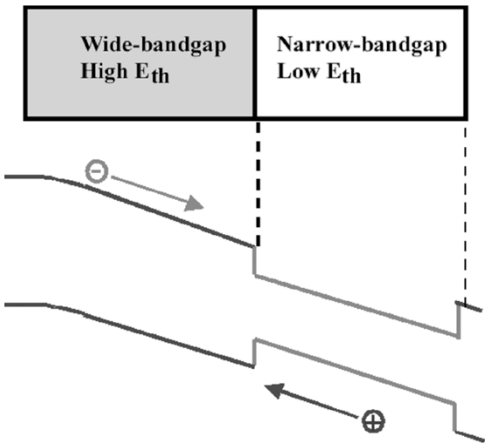

Fig. 3. Multiplication region of impact-ionization-engineered APD.

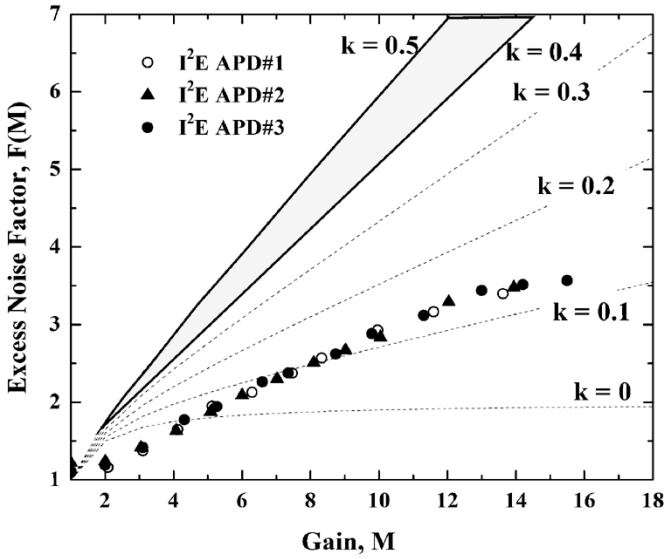

Fig. 4. Excess noise factor F(M) versus gain for an $In_{0.52}Ga_{0.15}Al_{0.33}As/In_{0.52}Al_{0.48}As$ I^2E APD.

p side of the cylindrical APD structure in [8], and the electric field profile in the intrinsic region has been calculated for with a Poisson solver. The simulated exponential-shaped gain curve (solid line) is consistent with experimental data [circles in Fig. 1(a)]. The simulated noise [Fig. 1(b)] is very low, as would be expected if $\beta \sim 0$.

It has also been shown for a wide range of materials including InP [12]–[15], GaAs [14]–[20], $Al_xIn_{1-x}As$ [14], [15], [21], Si [22], [23], $Al_xGa_{1-x}As$ [14], [15], [24]–[26], SiC [27], and GaInP [28] that lower excess noise and higher gain-bandwidth products can be achieved, irrespective of the value of k, by submicron scaling of the thickness of the multiplication region. The origin of this effect is the nonlocal nature of impact ionization, which is frequently expressed in terms of the so-called "dead space," the minimum distance over which carriers gain sufficient energy to impact ionize. The dead space effectively reduces the number of outlier high gain events [29], [30]. This, in turn, results in smaller deviations from the mean gain and, thus, lower excess noise factors. This is illustrated in Fig. 2, which shows the gain distributions of two $Al_{0.48}In_{0.52}As$ APDs with multiplication layer thickness of 1.0 (dashed line) and 0.1 μm (solid line). These APDs have the same average gain, M $\sim$ 20, but the excess noise factor was 6.9 and 4.0 for the 1.0- and 0.1–μm APDs, respectively. The gain distribution of the 1.0-μm APD is broader than the 0.1-μm device, which is an indication of higher multiplication noise. This graph also shows that the thicker device has higher probabilities for both high gain $(M > 80)$ and low gain $(M = 1)$ than the 0.1-μm APD, while the probabilities for the thin device are higher for gains in the range $2 < M < 80$. This is reasonable since they have different standard deviations in M while keeping $\langle M \rangle$ the same. It is interesting that the 1.0-μm APD has a peak at $M = 1$, while the 0.1 μm APD has a peak at $M = 2$. It follows, somewhat counter intuitively, that for the same gain, it is less likely that the initial carrier will emerge from the i-region without ionization for the thinner device. This has also been observed in [19].

A third approach that has achieved low noise is impact ionization engineering (I^2E) with beneficially designed heterostructures. This approach utilizes heterojunctions to provide greater localization of impact ionization than can be achieved in spatially uniform structures. Initial work that demonstrated the efficacy of this approach utilized the GaAs/$Al_xGa_{1-x}As$

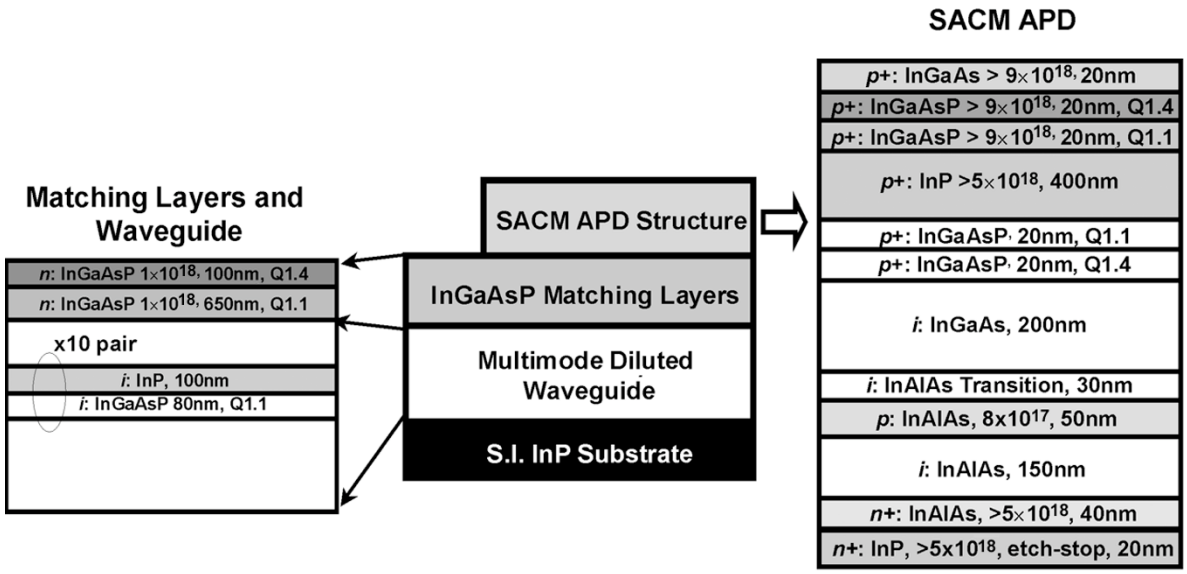

Fig. 5. Structure of evanescently-coupled waveguide APD.

material system. [31]–[35] More recently, InGaAlAs/InP implementations that operate at the telecommunications wavelengths have been reported. [36] The basic idea of I^2E is to place thin narrow bandgap layers with relatively low threshold energies adjacent to wider bandgap regions with higher threshold energies. An implementation of the I^2E structure is shown in Fig. 3. Structurally, the I^2E is similar to a truncated multiple quantum well (frequently mislabeled as "superlattice") APD [37], [38], however, operationally there is a fundamental difference in that the I^2E does not invoke heterojunction band discontinuities.

Fig. 4 shows the excess noise factor F(M) versus gain for three InGaAlAs I^2E APDs grown lattice-matched to InP by molecular beam epitaxy. [36] The unintentionally doped multiplication region, which consisted of a 100-nm-thick $In_{0.52}Al_{0.48}As$ layer and a 100-nm-thick $In_{0.52}Ga_{0.15}Al_{0.33}As$ quaternary layer, was sandwiched between p-type (3×10^{18} cm^{-3}, 0.8 μm), and n-type (5×10^{18} cm^{-3}, 0.5 μm) $In_{0.52}Al_{0.48}As$ layers, with a highly p-doped ($> 5 \times 10^{18}$ cm^{-3}, $\sim$30 nm) $In_{0.53}Ga_{0.47}As$ contact layer on the top. The lower bandgap energy of $In_{0.52}Ga_{0.15}Al_{0.33}As$ (estimated to be Eg $\sim$ 1.25 eV) as compared to $In_{0.52}Al_{0.48}As$ ($E_g \sim 1.51$ eV) results in lower carrier ionization threshold energy (E_{th}). There are relatively few ionization events in the $In_{0.52}Al_{0.48}As$ layer, owing to the combined effects of "dead space" and the higher threshold energy in $In_{0.52}Al_{0.48}As$. The dotted lines in Fig. 4 are plots of F(M) for k = 0 to 0.5 using the local field model [1], [2]. These plots are presented solely for reference because the k value has become a widely used figure of merit for excess noise. For $M \leq 4$, it appears that $k < 0$, which is unphysical and simply reflects the inapplicability of the local field model for this type of multiplication region. For higher gain, the excess noise is equivalent to a k value of $\sim$0.12. This is the lowest noise that has been reported for APDs that operate at the telecommunications wavelengths ($\lambda \sim$ 1300 nm and 1550 nm). For reference, the excess noise factor for commercial InP/$In_{0.53}Ga_{0.47}As$ APDs that have been widely deployed in fiber optic receivers is shown as the shaded region in Fig. 4. Typically, these APDs exhibit $0.4 < k < 0.5$.

An intuitive explanation of the I^2E APD is that carriers gain energy in the wide bandgap layer but since the threshold energy in that layer is relatively high, there are few ionization events. When the carriers enter the narrow bandgap layer, where the threshold energy is smaller, the energetic carriers ionize quickly. We conclude that the lower noise of the I^2E structure is a result of the spatial modulation of the probability distribution for impact ionization. The heterojunction results in a more spatially localized process, which, in turn, reduces the noise.

III. High-Speed APDs

For high-speed applications, it is essential for the APDs to achieve high gain-bandwidth products without sacrificing responsivity. At present, the most attractive approach to meeting these goals is to incorporate separate absorption, charge, and multiplication (SACM) APDs with the waveguide structures that have proved successful for high-speed p-i-n photodiodes. To date, a few edge-coupled waveguide APDs have been demonstrated [39]–[41]. High external quantum efficiency of 72% was achieved by direct edge coupling into the absorbing layer of 0.5-μm, but the bandwidth was only 20 GHz at low gain [39]. A similar approach with a thinner multiplication layer achieved a higher bandwidth of 35 GHz at low gain; the external quantum efficiency was 58% and the gain-bandwidth product was 140 GHz [40]. A higher gain-bandwidth product of 320 GHz was demonstrated with a thinner absorbing layer (0.2-μm), however the quantum efficiency was only 16% [41]. Using an APD with a 0.12-μm absorbing thickness, an evanescently-coupled asymmetric twin-waveguide APD obtained a quantum efficiency of 48% [42], but at the expense of a more complex (and thus more difficult to fabricate) structure. The bandwidth at low gain was 31.5 GHz and the gain-bandwidth product was 150 GHz.

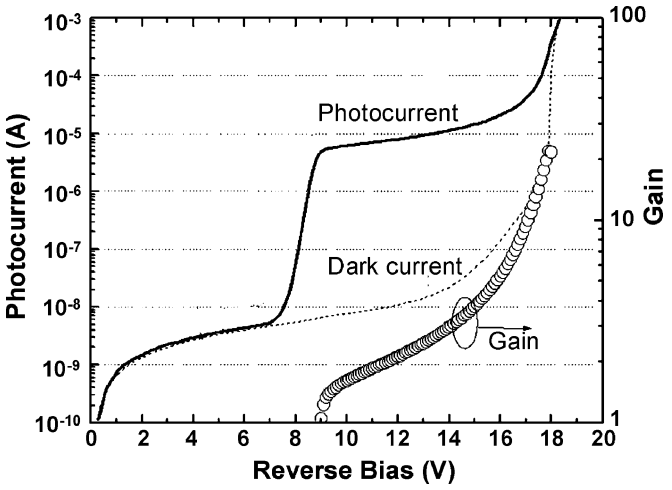

Fig. 6. Photocurrent, dark current, and gain of evanescently coupled waveguide APD.

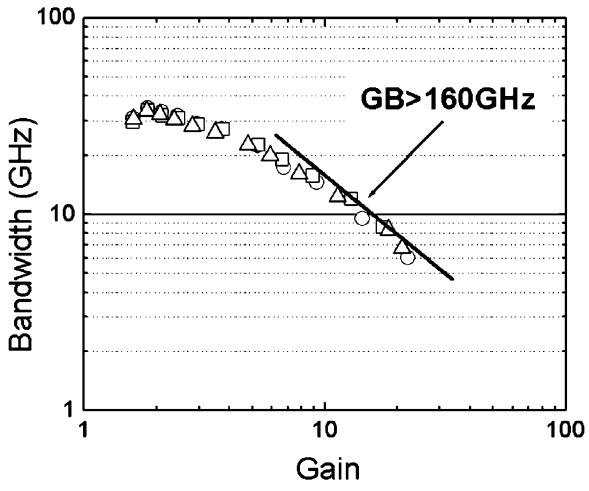

Fig. 7. Bandwidth versus gain for three evanescently-coupled waveguide APDs.

Previously, it has been shown that high efficiency (>80%) and broad bandwidth (>48 GHz) can be achieved with an evanescently coupled p-i-n having a planar short multimode input waveguide [43]. A strength of this approach is simplicity of fabrication. We have utilized this approach to fabricate an evanescently coupled waveguide SACM APD. A schematic cross section of the evanescently-coupled APD is shown in Fig. 5. The epitaxial structure was grown by low-pressure metal organic vapor phase epitaxy (LP-MOVPE) on semi-insulating InP substrate. The structure consists of a diluted waveguide and two optical matching layers [43] beneath the SACM APD. Proceeding sequentially from the bottom, the APD was comprised of an n-type AlInAs layer followed by an undoped AlInAs multiplication region of 150 nm. Then, a p-type AlInAs charge layer of 50 nm was grown with a nominal doping level of 8×10^{17} cm^{-3}. An undoped graded layer of 30 nm was inserted between the AlInAs charge layer and the InGaAs absorbing layer in order to smooth the heterojunction. Two 20-nm InGaAsP layers (1.4- and 1.1-μm bandgap) were used for the same purpose at the InGaAs/InP heterojunction. The absorbing layer thickness was 190-nm, which resulted in a total active SACM thickness of 0.46-μm. The associated short transit time enabled high-speed operation at low gains. Processing was similar to that for the p-i-n photodiodes described in [43].

Fig. 6 shows a typical current-voltage characteristic for a 5×20 μm^2 evanescently-coupled APD. The light was coupled from a 3-μm spotsize lensed fiber to the multimode waveguide. The capacitance-voltage characteristic indicated that the punchthrough voltage was ~10 V. The breakdown occurred below 18.5 V and the dark current at 90% of the breakdown was in the range 100–500 nA. To determine the gain at punchthrough, the quantum efficiency was measured using top illumination on a large-area device and was compared to the maximum theoretical value [41]. Following this method, the minimum gain at punchthrough was estimated to be 1.6.

The −3-dB bandwidths were measured with a heterodyne setup, based on the mixing of two single-mode DFB temperature-controlled lasers. Fig. 7 shows the −3 dB bandwidth versus dc gain achieved on 5×20 μm^2 photodiodes. The highest bandwidth of 34.8 GHz was obtained at 11 V reverse bias corresponding to a gain of 1.84. At the same gain, 5×15 and 5×30 μm^2 diodes exhibited bandwidths of 35.5 and 31.8 GHz, respectively, which suggests that the low-gain bandwidth was transit-time limited. At high gain, the bandwidth was limited by the gain-bandwidth, which was ~160 GHz.

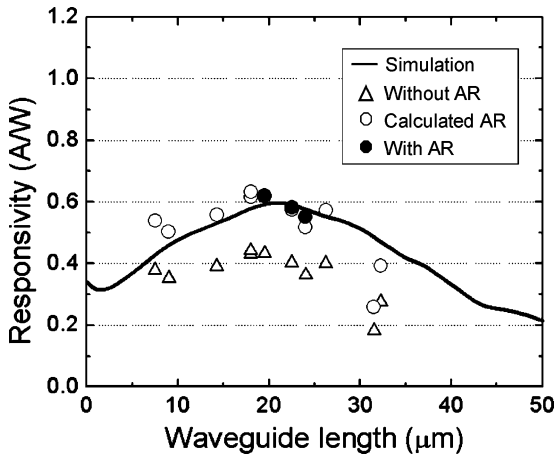

Fig. 8. Measured responsivity of evanescently-coupled waveguide APD with (●) and without (△) antireflection (AR) coating versus length of multimode input waveguide. Also shown are the calculated responsivity with AR coating (○) and BPM simulated response (solid line).

The thickness of the SACM layers were designed to obtain the best transfer of light from the input waveguide to the absorbing layer. The solid line in Fig. 8 presents the simulated responsivity of a 5×20 μm^2 diode versus the length of the multimode input waveguide. Owing to the low refractive index of the multiplication and charge layers, the projected responsivity was lower than for p-i-n photodiodes. In agreement with the modeling, the optimal waveguide length was 19 ± 1 μm. Using a 3-μm spotsize lensed fiber, a maximum responsivity of 0.62 A/W was achieved with AR coating at 1.543-μm wavelength with TE/TM polarization dependence less than 0.5 dB. The −1-dB alignment horizontal and vertical tolerances for a 5-μm-wide diode were ± 1.8 and ± 0.9 μm, respectively.

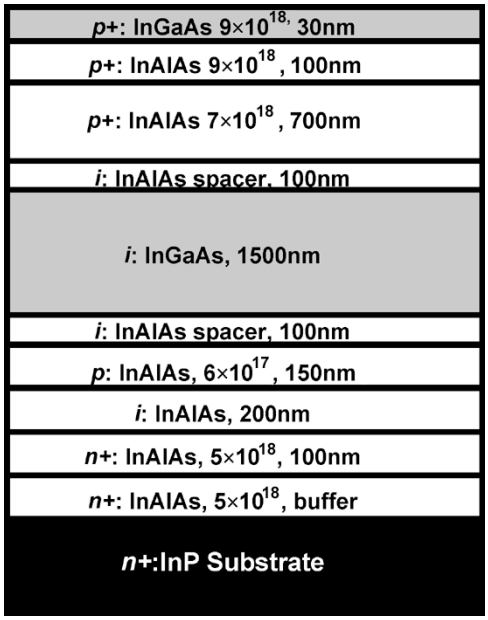

Fig. 9. Cross sectional schematic of $Al_{0.48}In_{0.52}As/In_{0.53}Ga_{0.47}As$ SACM structure utilized for the large-area APDs and arrays.

IV. Arrays and Large-Area APDs

Much of the research on III-V compound APDs has focused on achieving high-speed, low-noise operation for fiber optic receivers. For this application, small device size is preferred in order to reduce the RC time constant. On the other hand, emerging optical measurement systems that operate in the eye-safety wavelength range ($\sim$ 1.5 μm) require long-wavelength, high-sensitivity photodiodes with large detection area. For many applications of this type an APD is preferable to a p-i-n photodiode since the APD can achieve higher sensitivity. Similar material uniformity is required by APD imaging arrays [44]. Both applications present daunting challenges to the quality and uniformity of the epitaxial layers from which the APDs are fabricated. In response to these emerging applications, we have developed $Al_{0.48}In_{0.52}As/In_{0.53}Ga_{0.47}As$ APDs with diameters up to 500 μm and 18 $\times$ 18 arrays.

The SACM structure that was utilized for the large-area APDs and arrays is shown in Fig. 9. The APD wafers were grown by molecular beam epitaxy on n-type InP (100) substrates. Mesas were etched in phosphoric etchant ($H_3PO_4 : H_2O_2 : H_2O = 1 : 1 : 8$) to the n^+ InP buffer layer where a Ni (20)/AuGe (30)/Au (80 nm) n-type ohmic contact was formed. The Cr (25)/Au (85 nm) p-type contacts were formed by standard evaporation and lift off. APDs with a wide range of diameters (from 20 to 500 μm) were fabricated for characterization. Arrays of 50 μm-mesa-diameter APDs were also processed in order to evaluate the material quality, device uniformity, and device performance.

The typical photoresponse and dark current curves of a 500-μm-diameter APD are shown in Fig. 10. The punch-through voltage was $\sim$15.0 V, and the breakdown voltage was $\sim$39.2 V. The photocurrent was not flat above the punch-through voltage, an indication of gain prior to punch-through. The gain was estimated by comparing the measured external quantum efficiency with the theoretical

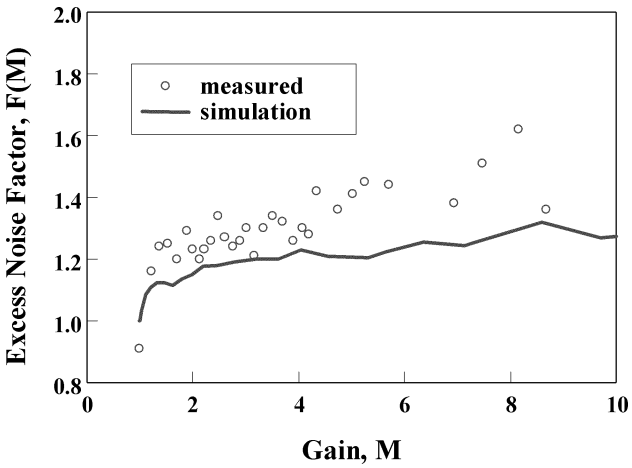

Fig. 10. Photocurrent, dark current, and gain curves for an $Al_{0.48}In_{0.52}As/In_{0.53}Ga_{0.47}As$ SACM APD.

maximum based on the reflected power at the surface and the thickness of the absorbing layer. This provided a lower limit to the gain. Using this approach the gain at 16.0 V was estimated to be $\sim$1.8. The assertion of gain at punch-through can be also corroborated by an estimate of the electric field intensity. At a reverse bias of 16.0 V, the electric field in the $In_{0.52}Al_{0.48}As$ multiplication region is $\sim$580 kV/cm, assuming a 200 nm $In_{0.52}Al_{0.48}As$ undoped multiplication region and a 150-nm p-type (6×10^{17} cm^{-3}) $In_{0.52}Al_{0.48}As$ charge region. This value of electric field is consistent with measurements on $In_{0.52}Al_{0.48}As$ homo-junction APDs [21], from which it was found that the electric field in a 200-nm-thick multiplication region at gain of 1.8 was $\sim$560 KV/cm.

The APD dark current consists of the bulk leakage current, which is proportional to the mesa area, and the sidewall leakage current, which scales with the mesa perimeter. The total dark current can be expressed as

$$I_{\text{total}} = J_{\text{sidewall}} \cdot \pi \cdot d + \frac{J_{\text{bulk}} \cdot \pi \cdot d^2}{4} \tag{1}$$

where J_{sidewall} is the sidewall leakage current density (in amps per micron) and J_{bulk} is the bulk leakage current density (in amps per micron squared). The measured dark current at bias voltage of $\sim$16 V is plotted in Fig. 11 versus mesa diameter. The solid line is a quadratic fit, which shows that the bulk component of the dark current is dominant. From the fit, the surface dark current density J_{sidewall} was 0.19 nA/μm and the bulk dark current density was 0.023 nA/μm^2. The total dark current can also be expressed in terms of the multiplied dark current and unmultiplied dark current using

$$I_{\text{total}} = I_{\text{unmultiplied}} + I_{\text{multiplied}} \cdot M. \tag{2}$$

By fitting the data to (2), it was found that the unmultiplied dark current (density) was $\sim$1.32 nA and the multiplied dark current was $\sim$1.54 nA. The dependence of dark current on gain remains linear to gain values $>$50. The low value of the unmultiplied dark current (density) is an indication of good material quality and surface passivation; it can be neglected for APDs biased at high gains.

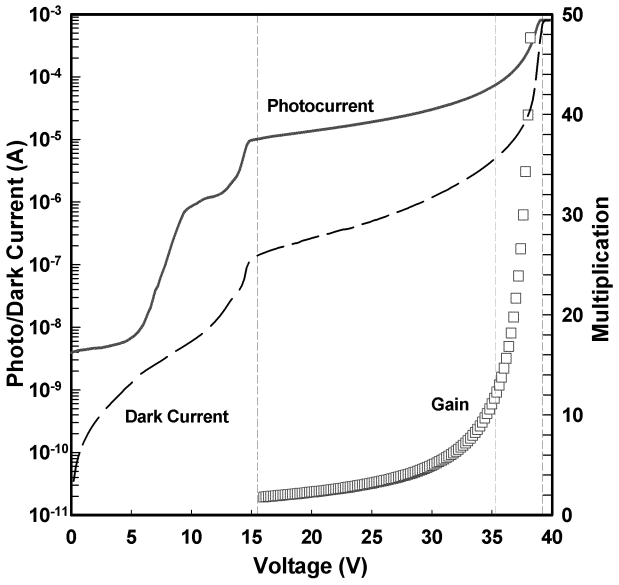

Fig. 11. Measured dark current and quadratic fit versus mesa diameter for $Al_{0.48}In_{0.52}As/In_{0.53}Ga_{0.47}As$ SACM APDs.

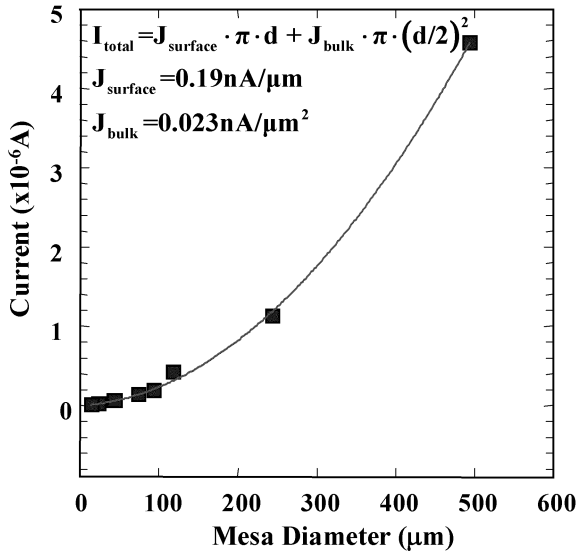

Fig. 12. Raster scan of photoresponse of a 500-μm-diameter $Al_{0.48}In_{0.52}As/In_{0.53}Ga_{0.47}As$ SACM APD for M $\sim$ 20.

The spatial uniformity of a 500-μm-diameter APD was measured by raster-scanning. A 1.52-μm-wavelength He–Ne laser beam with a beam-waist <5 μm across a 500-μm-diameter APD at M $\sim$20. A flat, uniform photoresponse profile was obtained across the whole mesa area, as shown in Fig. 12. No spikes in the interior or edge peaks were observed. The "hole" near the edge is due the probe and the top p-type contact.

The photocurrent, dark current, and gain of each device in an 18×18 array of 50-μm-diameter APDs were measured. Three devices on the array failed due to improper probing. Statistical analysis of the dark current for the other 321 devices exhibited a mean value of $\sim$4.4 nA and a standard deviation of 1.5 nA at the punchthrough voltage of 16.0 V (gain $\sim$1.8). The dark current distribution at 90% of the breakdown exhibited a mean value

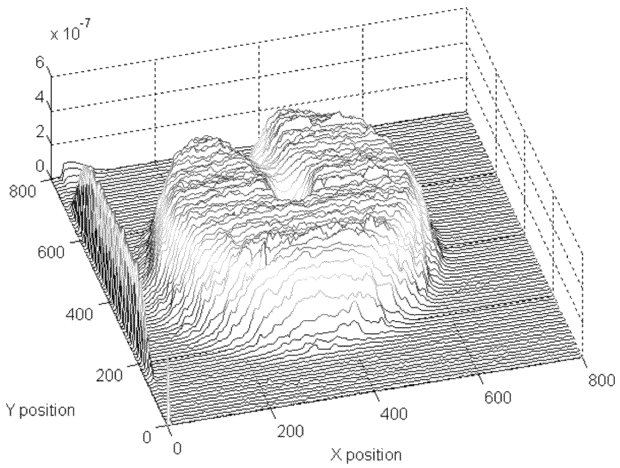

Fig. 13. Schematic cross section of 4H-SiC APD. The inset shows an SEM photograph of the etched mesa.

of $\sim$71 nA and a standard deviation of 13 nA. Uniform photocurrent was consistently observed across the array. The mean value of gain was 10.9, 16.1, 22.1, and 43.4 at reverse bias voltages of 35.0, 36.4, 37.2, and 38.2 V, respectively. The standard deviations of the gain distribution at each of these reverse bias conditions were 0.9, 1.4, 2.1, and 5.6, respectively. The low-gain bandwidth of one of the 50-μm-diameter APDs in the array was $\sim$8 GHz. The bandwidth at low gain was limited by the transit time through the long carrier transport path ($\sim$ 3.9 μm) associated with the depleted absorption, charge, and multiplication regions. At higher gains a gain-bandwidth product of 120 GHz was observed.

V. Ultraviolet (UV) APDs

Detection of UV light has numerous medical, military, and environmental applications. Photomultiplier tubes (PMTs) are frequently used for these applications because they have high responsivity (>600 A/W), high speed, and low dark current. However, they are costly, large, and require high bias voltages (typically several hundred volts). For some applications another major drawback to using PMTs is that expensive filters are required, due to their high response in the visible and near IR. Thus, it is desirable to replace PMTs with solid-state, UV photodetectors that have high gain. To this end, UV-enhanced Si APDs have been utilized with limited success. The Si APDs have the benefits of a mature material system, easy integration with integrated circuit technology, low noise, and good quantum efficiency. However, they have relatively high dark currents at room temperature and, like PMTs, require complex, expensive filters.

Back-illuminated solar-blind $Al_xGa_{1-x}N$ p-i-n's have recently demonstrated excellent performance ($D^* \sim 2 \times 10^{14}$ cmHz$^{1/2}$/W at 269 nm) with very low noise and strong rejection of wavelengths longer than 290 nm. [45] Typical responsivities at 280 nm were $\sim$0.12 A/W. GaN avalanche photodiodes (APDs) have been demonstrated [46]–[48], but the yields were very low due to defect-related micro-plasmas in the materials, and the devices were fragile and short-lived (typically a few minutes) [47], [48], which has precluded the development of APDs with acceptable performance.

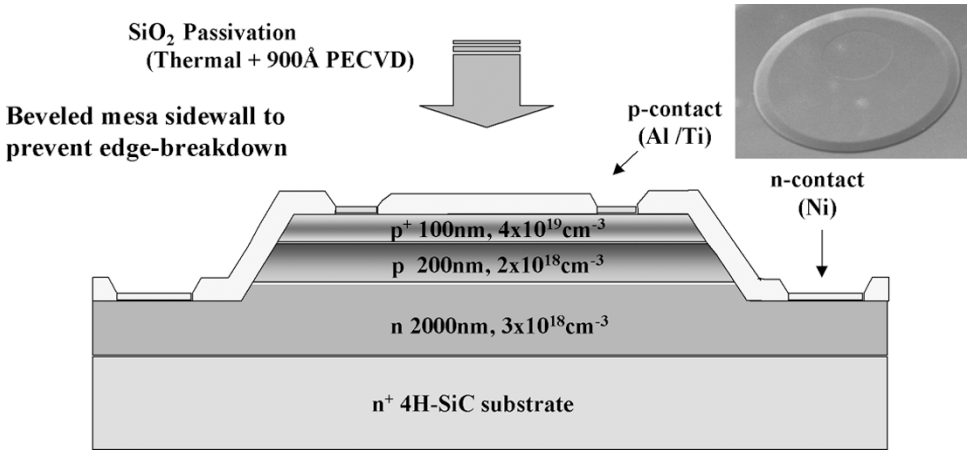

Fig. 14. Photocurrent, dark current, and gain of 100-μm-diameter 4H-SiC APD.

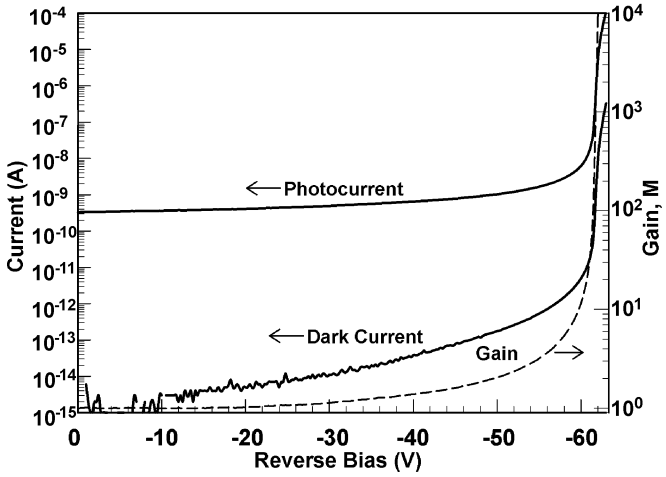

Fig. 15. Spectral response of 4H-SiC APD for a range of bias voltages.

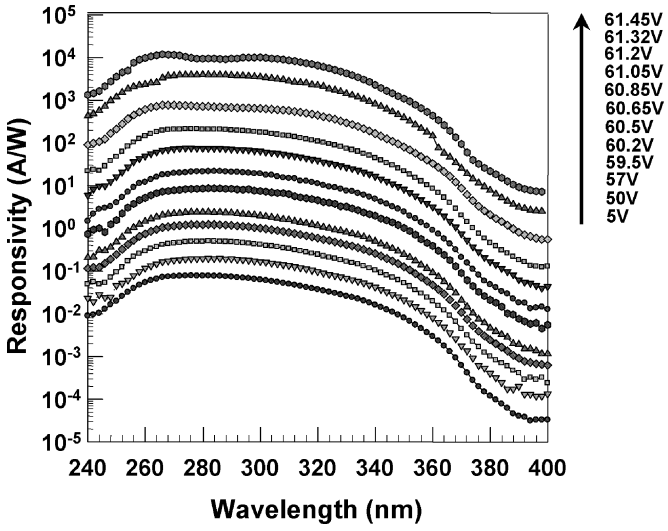

Fig. 16. Responsivity of 4H-SiC APD with and without a 266-nm "laser line" filter.

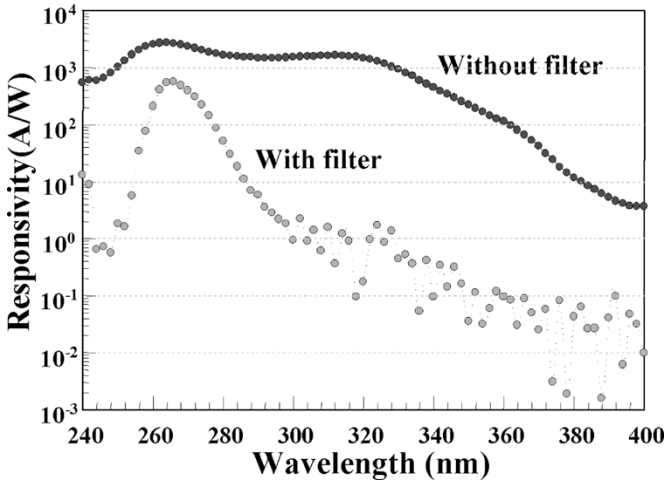

Fig. 17. Raster scans of the photocurrent of (a) nonbeveled and (b) beveled mesa-structure SiC APDs.

Recently, 4H-SiC avalanche photodiodes with strong UV responsivities (comparable to photomultipliers), low multiplication noise, and moderate bias voltages (<70 V) have been demonstrated [49]–[53]. Benefiting from an indirect wide band gap and its material maturity and stability, 4H-SiC is an attractive candidate for avalanche photodiodes. Konstantinov *et al.* have shown that 4H-SiC exhibits widely disparate ionization coefficients [54]. The low k value for hole initiated impact ionization and resulting low noise are advantageous for applications such as missile detection, laser-induced fluorescence biological-agent warning systems, and nonline-of-sight UV communications, for which low noise and high gain are crucial.

Fig. 13 shows the structure of a SiC APD grown on n^+ 4H-SiC substrate. It consists of a 0.1-μm p^+ cap layer, a 0.2-μm p layer, and a 2-μm n layer. Mesas were defined by reactive ion etching (RIE), with BCl_3, to the underlying n layer. The sidewall passivation was achieved by 750 °C thermal oxidation in a wet oxidation furnace for 4 h. P-type (Al/Ti) contacts and n-type (Ni) contacts were patterned and deposited by a standard liftoff process. Both contacts were annealed in an RTA at 850 °C for 6 min in N_2.

Fig. 14 shows the reverse current-voltage characteristics of a typical 100-μm-diameter device. The devices exhibited an abrupt uniform breakdown near 61 V. In order to determine the gain, the photocurrent at -5 V was used as the unity gain reference point. Above this voltage, a slight linear increase in the photocurrent with bias is observed. It has been shown that

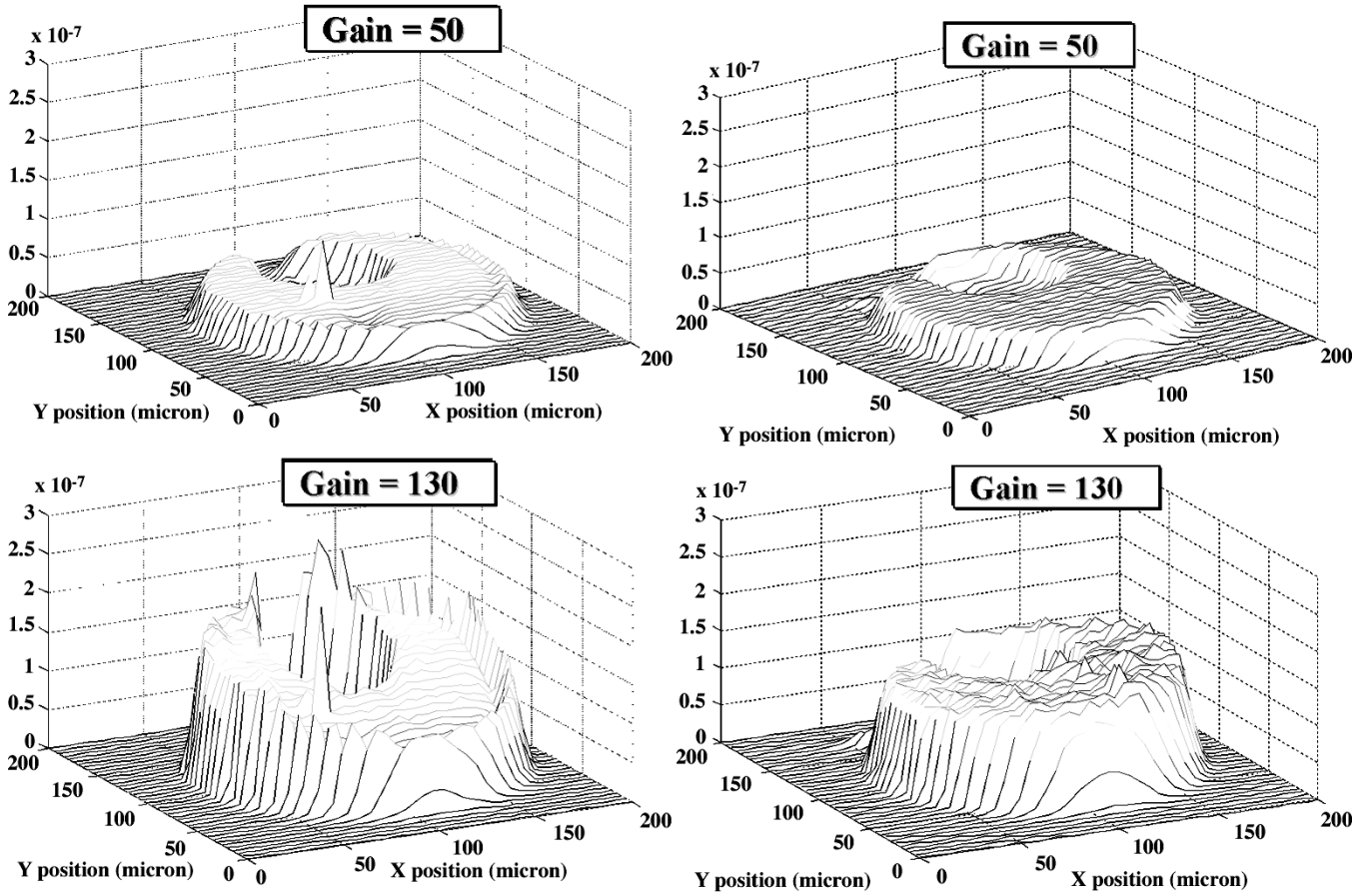

Fig. 18. Measured excess noise, F(M), of a SiC APD versus gain, M. The excess noise corresponds to a k value of 0.15.

this slope in the photocurrent is due to slight widening of the depletion region [55]. A linear correction to account for this has been used for the gain determination. Below 30 V, the dark current was $<$10 fA and for photocurrent gain $\sim 10^3$, the dark current was $<$0.87 nA. The average dark current density at 95% of breakdown was 32 nA/cm^2.

The spectral response for a range of bias voltages is shown in Fig. 15. The response begins to cut off at 380 nm, corresponding to the 3.26-eV bandgap of 4H-SiC. The long-wavelength cutoff is not as sharp as that of direct bandgap semiconductors such as GaN. Nevertheless, the response drops by almost three orders of magnitude between 320 and 400 nm, providing a good visible blind response. At unity gain, the external quantum efficiency was $\sim$35% at 276 nm (responsivity $= 78$ mA/W). As the bias increased toward breakdown, the responsivity increased by over five orders of magnitude; the peak responsivity was greater than 10 000 A/W at 266 nm. For applications that require a true solar-blind response, utilization of a SiC APD will require an external filter. Fig. 16 shows the responsivity with a "laser line" filter having a center wavelength of 266 nm. A sharp narrowband response with a peak responsivity of $\sim$800 A/W was observed.

At very high gains, spatial uniformity of the photoresponse becomes a critical issue. Small variations in the electric field whether structural or materials in origin can result in large "gain spikes." For mesa structure SiC APDs, breakdown tends to occur at the mesa edge for negative bevel angles and steep positive bevels [56]. This can be suppressed by fabricating very shallow ($\leq 7^\circ$) positive bevels. [57] This is illustrated by the two-dimensional raster scans of the photoresponse of nonbeveled and beveled SiC APDs in Fig. 17(a) and (b). The beveled sample had a bevel angel of approximately 7° while the nonbeveled device showed no discernible bevel angle, indicating $\sim 90^\circ$ sidewall. For both types of devices, the scans at unity gain (5-V reverse bias) exhibit a flat, uniform response. The circular gaps near the rear are the top p-type contacts, which shield the incident light. Fig. 17(a) shows photocurrent scans for a nonbeveled device at gains of 50 and 130. At a gain of 50, edge breakdown begins around the edges of the device. This becomes more pronounced at a gain of 130. The increased response occurring behind the contact, toward the device edge, results primarily from field crowding. The beveled device [Fig. 17(b)], on the other hand, shows no evidence of edge breakdown at gains of 50 and 130. The luminescence of the beveled device at breakdown (current density > 1.5 A/cm^2) was uniform, and indication bulk breakdown.

It is well known that multiplication dominated by a single carrier type, either an electron or a hole, has better noise performance than devices with equal multiplication events of both carrier types. Fig. 18 shows the measured excess noise factors of a SiC APD as a function of gain. The excess noise of the device corresponds to a k value of 0.15.

An upper-bound of detectivity D* can be estimated by assuming that the device is thermal noise limited at zero bias.

In that case, the spectral density of the noise current S_n is given by $S_n = 4k_BT/R_0$, where $R_0 = (dV/dI)_{V=0}$, k_B is Bolzman's constant, and T is temperature. Accordingly, D* is given by $D^* = \Re\sqrt{R_0A_D/4k_bT}$, where $\Re$ is the responsivity and A_D is the cross-sectional area of the photodetector. Curve fitting to the current-voltage characteristic of a 480-μm-diameter device yielded $R_0 = 3.7 \times 10^{15}\ \Omega$. Details of the curve-fitting procedure can be found in [58]. Consequently, an upper-bound of D* was estimated to be 1.6×10^{15} cm·Hz$^{1/2}$/W at 276 nm.

VI. Conclusion

Optical receivers for telecommunications has pushed the development of APDs with high bandwidth, low excess noise, and high gain bandwidth products. It has been shown that lower noise and higher gain bandwidth products can be achieved by submicron scaling of the multiplication region thickness and replacing InP in the multiplication layer with $Al_{0.48}In_{0.52}As$. We project that impact ionization engineering with beneficially designed heterostructures can reduce the noise even further. High-speed operation can achieved with waveguide structures. We have described an evanescently-coupled APD structure with a short multimode input waveguide section that is easy to fabricate. These APDs have demonstrated bandwidths >30 GHz, responsivity of 0.6 A/W at 1.55 μm, and gain-bandwidth product of 160 GHz. For high-sensitivity infrared imaging applications, HgCdTe APDs have achieved extremely low noise consistent with single carrier multiplication. Through Monte Carlo modeling, we have shown that this can be explained to a great extent through consideration of the bandstructure of HgCdTe. SiC APDs appear to be promising candidates for UV sensing. We report gains of 10^4, low dark current, and low excess noise ($k \sim 0.15$), however, spatial uniformity of the photoresponse at very high gains remains work in progress.

References

[1] R. J. McIntyre, "Multiplication noise in uniform avalanche diodes," *IEEE Trans. Electron Devices*, vol. ED-13, pp. 164–168, Jan. 1966.

[2] ——, "The distribution of gains in uniformly multiplying avalanche photodiodes: Theory," *IEEE Trans. Electron Devices*, vol. ED-19, pp. 703–713, 1972.

[3] R. B. Emmons, "Avalanche-photodiode frequency response," *J. Appl. Phys.*, vol. 38, no. 9, pp. 3705–3714, 1967.

[4] B. K. Ng, J. P. R. David, R. C. Tozer, M. Hopkinson, G. Hill, and G. J. Rees, "Excess noise characteristics of $Al_{0.8}Ga_{0.2}As$ avalanche photodiodes," *IEEE Photon. Tech. Lett.*, vol. 14, pp. 522–524, Apr. 2002.

[5] X. G. Zheng, X. Sun, S. Wang, P. Yuan, G. S. Kinsey, A. L. Holmes, Jr., B. G. Streetman, and J. C. Campbell, "Multiplication noise of $Al_xGa_{1-x}As$ avalanche photodiodes with high Al concentration and thin multiplication region," *Appl. Phys. Lett.*, vol. 78, pp. 3833–3835, 2001.

[6] B. K. Ng, J. P. R. David, G. J. Rees, R. C. Tozer, M. Hopkinson, and R. J. Airey, "Avalanche multiplication and breakdown in $Al_xGa_{1-x}As$ ($x < 0.9$)," *IEEE Trans. Electron Dev.*, vol. 49, pp. 2349–2351, Feb. 2002.

[7] J. D. Beck, C. F. Wan, M. A. Kinch, and J. E. Robinson, "MWIR HgCdTe avalanche photodiodes," *Proc. SPIE, Materials for Infrared Detectors*, vol. 4454, pp. 188–197, 2001.

[8] A. Chen and A. Sher, "CPA band calculation for (Hg, Cd)Te," *J. Vac. Sci. Technol.*, vol. 21, pp. 138–141, 1982.

[9] R. W. Miles, C. L. Jones, J. C. Brice, and P. Capper, *Properties of Mercury Cadmium Telluride*, J. Brice and P. Capper, Eds. London, U.K.: INSPEC, 1987, p. 101.

[10] L. V. Keldysh, *Sov. Phys.—JETP*, vol. 10, p. 509, 1960.

[11] C. L. Anderson and C. R. Crowell, "Threshold energies of electron-hole pair production by impact ionization in semiconductors," *Phys. Rev. B, Condens. Matter*, vol. 5, pp. 2267–2272, 1972.

[12] K. F. Li, S. A. Plimmer, J. P. R. David, R. C. Tozer, G. J. Rees, P. N. Robson, C. C. Button, and J. C. Clark, "Low avalanche noise characteristics in thin InP p^+-i-n^+ diodes with electron initiated multiplication," *IEEE Photon. Tech. Lett.*, vol. 11, pp. 364–366, Mar. 1999.

[13] J. C. Campbell, S. Chandrasekhar, W. T. Tsang, G. J. Qua, and B. C. Johnson, "Multiplication noise of wide-bandwidth InP/InGaAsP/InGaAs avalanche photodiodes," *J. Lightwave Technol.*, vol. 7, pp. 473–477, Mar. 1989.

[14] P. Yuan, C. C. Hansing, K. A. Anselm, C. V. Lenox, H. Nie, A. L. Holmes, Jr., B. G. Streetman, and J. C. Campbell, "Impact ionization characteristics of III-V semiconductors for a wide range of multiplication region thicknesses," *IEEE J. Quantum Electron.*, vol. 36, pp. 198–204, Feb. 2000.

[15] M. A. Saleh, M. M. Hayat, P. O. Sotirelis, A. L. Holmes, J. C. Campbell, B. Saleh, and M. Teich, "Impact-ionization and noise characteristics of thin III-V avalanche photodiodes," *IEEE Trans. Electron Devices*, vol. 48, pp. 2722–2731, Dec. 2001.

[16] K. F. Li, D. S. Ong, J. P. R. David, R. C. Tozer, G. J. Rees, S. A. Plimmer, K. Y. Chang, and J. S. Roberts, "Avalanche noise characteristics of thin GaAs structures with distributed carrier generation," *IEEE Trans. Electron Devices*, vol. 47, pp. 910–914, May 2000.

[17] K. F. Li, D. S. Ong, J. P. R. David, G. J. Rees, R. C. Tozer, P. N. Robson, and R. Grey, "Avalanche multiplication noise characteristics in thin GaAs p^+-i-n^+ diodes," *IEEE Trans. Electron Dev.*, vol. 45, pp. 2102–2107, Oct. 1998.

[18] C. Hu, K. A. Anselm, B. G. Streetman, and J. C. Campbell, "Noise characteristics of thin multiplication region GaAs avalanche photodiodes," *Appl. Phys. Lett.*, vol. 69, no. 24, pp. 3734–3736, 1996.

[19] D. S. Ong, K. F. Li, G. J. Rees, G. M. Dunn, J. P. R. David, and P. N. Robson, "A Monte Carlo investigation of multiplication noise in thin $p^+ - i - n^+$ GaAs avalanche photodiodes," *IEEE Trans. Electron Dev.*, vol. 45, pp. 1804–1810, Aug. 1998.

[20] S. A. Plimmer, J. P. R. David, D. C. Herbert, T.-W. Lee, G. J. Rees, P. A. Houston, R. Grey, P. N. Robson, A. W. Higgs, and D. R. Wight, "Investigation of impact ionization in thin GaAs diodes," *IEEE Trans. Electron Dev.*, vol. 43, pp. 1066–1072, July 1996.

[21] C. Lenox, P. Yuan, H. Nie, O. Baklenov, C. Hansing, J. C. Campbell, and B. G. Streetman, "Thin multiplication region InAlAs homojunction avalanche photodiodes," *Appl. Phys. Lett.*, vol. 73, pp. 783–784, 1998.

[22] C. H. Tan, J. C. Clark, J. P. R. David, G. J. Rees, S. A. Plimmer, R. C. Tozer, D. C. Herbert, D. J. Robbins, W. Y. Leong, and J. Newey, "Avalanche noise measurements in thin Si $p^+ - i - n^+$ diodes," *Appl. Phys. Lett.*, vol. 76, no. 26, pp. 3926–3928, 2000.

[23] C. H. Tan, J. P. R. David, J. Clark, G. J. Rees, S. A. Plimmer, D. J. Robbins, D. C. Herbert, R. T. Carline, and W. Y. Leong, "Avalanche multiplication and noise in submicron Si p-i-n diodes," *Proc. SPIE, Silicon-Based Optoelectronics II*, vol. 3953, pp. 95–102, 2000.

[24] B. K. Ng, J. P. R. David, G. J. Rees, R. C. Tozer, M. Hopkinson, and R. J. Riley, "Avalanche multiplication and breakdown in $Al_xGa_{1-x}As$ ($x < 0.9$)," *IEEE Trans. Electron Devices*, vol. 49, pp. 2349–2351, Dec. 2002.

[25] B. K. Ng, J. P. R. David, R. C. Tozer, M. Hopkinson, G. Hill, and G. H. Rees, "Excess noise characteristics of $Al_{0.8}Ga_{0.2}As$ avalanche photodiodes," *IEEE Photon. Tech. Lett.*, vol. 14, pp. 522–524, Apr. 2002.

[26] C. H. Tan, J. P. R. David, S. A. Plimmer, G. J. Rees, R. C. Tozer, and R. Grey, "Low multiplication noise thin Al0.6Ga0.4As avalanche photodiodes," *IEEE Trans. Electron Devices*, vol. 48, pp. 1310–1317, July 2001.

[27] B. K. Ng, J. P. R. David, R. C. Tozer, G. J. Rees, Y. Feng, J. H. Zhao, and M. Weiner, "Nonlocal effects in thin 4H-SiC UV avalanche photodiodes," *IEEE Trans. Electron Devices*, vol. 50, pp. 1724–1732, Aug. 2003.

[28] C. H. Tan, R. Ghin, J. P. R. David, G. J. Rees, and M. Hopkinson, "The effect of dead space on gain and excess noise in $In_{0.48}Ga_{0.52}P$ p^+in^+ diodes," *Semicon. Sci. Technol.*, vol. 18, no. 8, pp. 803–806, 2003.

[29] D. S. Ong, K. F. Li, G. J. Rees, G. M. Dunn, J. P. R. David, and P. N. Robson, "A Monte Carlo investigation of multiplication noise in thin $p^+ - i - n^+$ GaAs avalanche photodiodes," *IEEE Trans. Electron Devices*, vol. 45, pp. 1804–1809, Aug. 1998.

[30] X. Li, X. Zheng, S. Wang, F. Ma, and J. C. Campbell, "Calculation of gain and noise with dead space for GaAs and $Al_xGa_{1-x}As$ avalanche photodiodes," *IEEE Trans. Electron Devices*, vol. 49, pp. 1112–1117, July 2002.

[31] P. Yuan, S. Wang, X. Sun, X. G. Zheng, A. L. Holmes, Jr., and J. C. Campbell, "Avalanche photodiodes with an impact-ionization-engineered multiplication region," *IEEE Photon. Technol. Lett.*, vol. 12, pp. 1370–1372, Oct. 2000.

[32] S. Wang, R. Sidhu, X. G. Zheng, X. Li, X. Sun, A. L. Holmes, Jr., and J. C. Campbell, "Low-noise avalanche photodiodes with graded impact-ionization-engineered multiplication region," *IEEE Photon. Technol. Lett.*, vol. 13, pp. 1346–1348, Dec. 2001.

[33] S. Wang, F. Ma, X. Li, R. Sidhu, X. G. Zheng, X. Sun, A. L. Holmes, Jr., and J. C. Campbell, "Ultra-low noise avalanche photodiodes with a "centered-well" multiplication region," *IEEE J. Quantum Electron.*, vol. 39, pp. 375–378, Feb. 2003.

[34] O.-H. Kwon, M. M. Hayat, S. Wang, J. C. Campbell, A. L. Holmes, Jr., B. E. A. Saleh, and M. C. Teich, "Optimal excess noise reduction in thin heterojunction $Al_{0.6}Ga_{.4}As-GaAs$ avalanche photodiodes," *IEEE J. Quantum Electron.*, vol. 39, pp. 1287–1296, Oct. 2003.

[35] M. M. Hayat, O.-H. Kwon, S. Wang, J. C. Campbell, B. E. A. Saleh, and M. C. Teich, "Boundary effects on multiplication noise in thin heterostructure avalanche photodiodes: Theory and experiment," *IEEE Trans. Electron Dev.*, vol. 49, pp. 2114–2123, Dec. 2002.

[36] S. Wang, J. B. Hurst, F. Ma, R. Sidhu, X. Sun, X. G. Zheng, A. L. Holmes, Jr., J. C. Campbell, A. Huntington, and L. A. Coldren, "Low-noise impact-ionization-engineered avalanche photodiodes grown on InP substrates," *IEEE Photon. Tech. Lett.*, vol. 14, pp. 1722–1724, Dec. 2002.

[37] F. Capasso, W. T. Tsang, A. L. Hutchinson, and G. F. Williams, "Enhancement of electron impact ionization in a superlattice: A new avalanche photodiode with a large ionization rate ratio," *Appl. Phys. Lett.*, vol. 40, pp. 38–40, 1982.

[38] R. Chin, N. Holonyak, Jr., G. E. Stillman, J. Y. Tang, and K. Hess, "Impact ionization in multilayered heterojunction structures," *Electron. Lett.*, vol. 16, pp. 467–469, 1980.

[39] C. Cohen-Jonathan, L. Giraudet, A. Bonzo, and J. P. Praseuth, "Waveguide AlInAs/GaAlInAs avalanche photodiode with a gain-bandwidth product over 160 GHz," *Electron. Lett.*, vol. 33, pp. 1492–1493, 1997.

[40] T. Nakata, T. Takeuchi, K. Makita, and T. Torikai, "High-speed and high-sensitivity waveguide InAlAs avalanche photodiode for 10–40 Gb/s receivers," in *Proc. Laser Electro-Optical Soc.*, 2001, paper ThN3.

[41] G. S. Kinsey, J. C. Campbell, and A. G. Dentai, "Waveguide avalanche photodiode operating at 1.55 μm with a gain-bandwidth product of 320 GHz," *IEEE Photonics Tech. Lett.*, vol. 13, pp. 842–844, Aug. 2001.

[42] J. Wei, F. Xia, and S. R. Forest, "A high-responsivity high-bandwidth asymmetric twin-waveguide coupled InGaAs-InP-InAlAs avalanche photodiode," *IEEE Photon. Technol. Lett.*, vol. 14, pp. 1590–1592, 2002.

[43] S. Demiguel, N. Li, X. Li, X. Zheng, J. Kim, J. C. Campbell, H. Lu, and K. A. Anselm, "Very high-responsivity evanescently-coupled photodiodes integrating a short planar multimode waveguide for high-speed applications," *IEEE Photon. Technol. Lett.*, vol. 15, pp. 1761–1763, Dec. 2003.

[44] M. J. Lange, J. C. Dries, and W. Huang, "Confocal SWIR and 3D range finding using InGaAs P-I-N and APD detector arrays," in *Proc. Laser Electro-Optical Soc. Annu. Meet.*, Tucson, AZ, 2003, pp. 688–689.

[45] C. J. Collins, U. Chowdhury, M. M. Wong, B. Yang, A. L. Beck, R. D. Dupuis, and J. C. Campbell, "Improved solar-blind detectivity using an $Al_xGa_{1-x}N$ heterojunction p-i-n photodiode," *Appl. Phys. Lett.*, vol. 80, pp. 3754–3756, 2002.

[46] K. A. McIntosh, R. J. Molnar, L. J. Mahoney, A. Lightfoot, M. W. Geis, K. M. Molvar, I. MeIngailis, R. L. Aggarwal, W. D. Goodhue, S. S. Choi, D. L. Spears, and S. Verghese, "GaN avalanche photodiodes grown by hydride vapor-phase epitaxy," *Appl. Phys. Lett.*, vol. 75, pp. 3485–3487, 1999.

[47] J. C. Carrano, D. J. H. Lambert, C. J. Eiting, C. J. Collins, T. Li, S. Wang, B. Yang, A. L. Beck, R. D. Dupuis, and J. C. Campbell, "GaN avalanche photodiodes," *Appl. Phys. Lett.*, vol. 76, pp. 924–926, 2000.

[48] B. Yang, T. Li, K. Heng, C. Collins, S. Wang, J. C. Carrano, R. D. Dupuis, J. C. Campbell, M. J. Schurman, and I. T. Ferguson, "Low dark current GaN avalanche photodiodes," *IEEE J. Quantum Electron.*, vol. 36, pp. 1389–1391, Dec. 2000.

[49] F. Yan, Y. Luo, J. H. Zhao, and G. H. Olsen, "4H-SiC visible blind UV avalanche photodiodes," *Electron Lett.*, vol. 35, pp. 929–930, 1999.

[50] B. K. Ng, F. Yan, J. P. R. David, R. C. Tozer, G. J. Rees, C. Qin, and J. H. Zhao, "Multiplication and excess noise characteristics of thin 4H-SiC UV avalanche photodiodes," *IEEE Photon. Technol. Lett.*, vol. 14, pp. 1342–1344, Sept. 2002.

[51] B. K. Ng, J. P. R. David, R. C. Tozer, G. J. Rees, F. Yan, and M. Weiner, "Nonlocal effects in thin 4H-SiC UV avalanche photodiodes," *IEEE Trans. Electron Devices*, vol. 50, pp. 1724–1732, Aug. 2003.

[52] F. Yan, J. H. Zhao, and G. Olsen, "Demonstration of the first 4H-SiC avalanche photodiodes," *Solid State Electron.*, vol. 44, pp. 341–346, 2000.

[53] X. Guo, A. Beck, B. Yang, and J. C. Campbell, "Low dark current 4H-SiC avalanche photodiodes," *Electron. Lett.*, vol. 39, no. 23, pp. 1673–1674, 2003.

[54] A. O. Konstantinov, Q. Wahab, N. Nordell, and U. Lindefelt, "Ionization rates and critical fields in 4H silicon carbide," *Appl. Phys. Lett.*, vol. 71, pp. 90–92, 1997.

[55] S. Wang, R. Sidhu, G. Karve, F. Ma, X. Li, X. Zheng, J. B. Hurst, X. Sun, N. Li, A. L. Holmes, Jr., and J. C. Campbell, "A study of low-bias photocurrent gradient of avalanche photodiodes," *IEEE Trans. Electron. Devices*, vol. 49, pp. 2107–2113, 2002.

[56] B. J. Baliga, *Power Semiconductor Devices*. Boston, MA: PWS, 1995.

[57] F. Yan, C. Qin, J. H. Zhao, M. Weiner, B. K. Ng, J. P. R. David, and R. C. Tozer, "Low-noise visible-blind UV avalanche photodiodes with edge terminated by 2° positive bevel," *Electron. Lett.*, vol. 38, pp. 335–336, 2002.

[58] C. J. Collins, T. Li, D. J. H. Lambert, M. M. Wong, R. D. Dupuis, and J. C. Campbell, "Selective regrowth of $Al_{0.30}Ga_{0.70}N$ p-i-n photodiodes," *Appl. Phys. Lett.*, vol. 77, pp. 2810–2812, 2000.

Joe C. Campbell (S'73–M'74–SM'88–F'90) received the B.S. degree in physics from the University of Texas at Austin in 1969, and the M.S. and Ph.D. degrees in physics from the University of Illinois at Urbana-Champaign in 1971 and 1973, respectively.

From 1974 to 1976, he was with Texas Instruments, where he worked on integrated optics. In 1976, he joined the staff of AT&T Bell Laboratories, Holmdel, NJ. In the Crawford Hill Laboratory, he worked on a variety of optoelectronic devices including semiconductor lasers, optical modulators, waveguide switches, photonic integrated circuits, and photodetectors with emphasis on high-speed avalanche photodiodes for high-bit-rate lightwave systems. In January 1989, he joined the faculty of the University of Texas at Austin as Professor of Electrical and Computer Engineering and Cockrell Family Regents Chair in Engineering. At present, he is actively involved in Si-based optoelectronics, high-speed, low-noise avalanche photodiodes, high-power photodiodes, ultraviolet photodetectors, and quantum-dot IR imaging. He has coauthored six book chapters, more than 300 journal publications, and 200 conference presentations.

Prof. Campbell is a member of the National Academy of Engineering, a Fellow of the Optical Society of America, and a Fellow of the American Physical Society.

Stephane Demiguel was born in Gennevilliers, France, in 1971. He received the engineer degree in electrical engineering from Ecole Supirieure d'Ingenieurs en Ginie Electrique (ESIGELEC), Rouen, France, in 1996, and the Ph.D. degree in optoelectronics from Rouen University, Rouen, France, in 2001. His Ph.D. dissertation was on high-speed photodiodes integrating spot size converter for 60-GHz radio over fiber links and 40-Gb/s optical transmissions.

In 2000, he worked on the design and measurements of high-speed photodiodes at Alcatel Opto+, Marcoussis, France. In particular, he was involved in optical and electrical modeling for optoelectronic devices. In 2002, he joined Prof. Joe Campbell's group at the University of Texas at Austin. He is currently working on high-speed PIN, APD, and high-power photodiodes utilizing an evanescently-coupled approach integrating a multimode waveguide.

Feng Ma was born in Beiyang, China, on April 18, 1973. He received the B.S. degree in applied physics from Beijing Institute of Technology, Beijing, China, in 1991, the M.S. degree in theoretical physics from Beijing Normal University, Beijing, in 1994, and the M.A. and Ph.D. degrees in astronomy and the Ph.D. degree in electrical engineering from the University of Texas at Austin in 1997, 2000, and 2001, respectively.

Ariane Beck received the B.S. and M.S. degrees in electrical and computer engineering from the University of Texas at Austin in 2000 and 2002, respectively. Currently, she is working toward the Ph.D. degree in electrical engineering at the Microelectronics Research Center at the University of Texas at Austin. Her research focuses on wide-bandgap ultraviolet photodetectors.

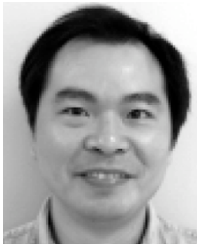

Xiangyi Guo received the B.S. and M.S. degrees from the Physics Department of East China Normal University, Shanghai, China, in 1991 and 1997, respectively. He is currently pursuing the Ph.D. degree in electrical engineering at the University of Texas at Austin.

He was with Shanghai Institute of Technical Physics, Chinese Academy of Sciences, from 1994 to 1996, working on solar radiation detection. From 1997 to 2001, he was with Philips Optical Storage, Shanghai, where he was engaged in the application of optical storage devices. His research interests are wide-bandgap optoelectronic devices.

Shuling Wang received the B. S. degree in microelectronics from Beijing University, Beijing, China in 1995, the M.S.E.E. degree from the University of Notre Dame in 1999, and the Ph.D. degree in electrical engineering from the University of Texas at Austin in 2002.

She is currently a Research Scientist in the Microelectronics Research Center at the University of Texas working on high-speed, low-noise avalanche photodiodes.

Dr. Wang is a member of the IEEE Laser and Electro-Optics Society (LEOS).

Xiaoguang Zheng received the B.S.E.E. degree from the Beijing Institute of Technology, Beijing, China, in 1985, the M.S. degree in electrical engineering from the Hebei Semiconductor Research Institute in 1991, and the Ph.D. degree in electrical engineering from the University of Texas at Austin in 2003.

His major research interests are in optoelectronic devices: impact ionization properties of III-V compound materials, high-speed long-wavelength avalanche photodiodes and arrays, and heterogeneous material integration via direct wafer bonding.

Xiaowei Li was born in Beijing, China, in 1970. He received the B.S. and M.S. degrees from the Physics Department of Peking University, Beijing, China, in 1994 and 1997, respectively. He is currently pursuing the Ph.D. degree in electrical engineering from the Microelectronic Research Center at the University of Texas at Austin.

His research interests are avalanche process simulations and high saturation power photodetectors for 1.55-μm applications.

Jeffrey D. Beck (S'69–M'72) received the S.B and S.M. degrees in electrical engineering from the Massachusetts Institute of Technology, Cambridge, in 1972.

He is a Distinguished Member of the Technical Staff in the Research and Development group at DRS Infrared Technologies, Dallas, TX. He has over 35 years of experience in infrared technology. He began his career in the infrared in 1968 as an MIT Electrical Engineering intern working for Honeywell Radiation Center in Lexington, MA, where he was employed until 1978. In 1978, he relocated to Dallas to accept a position as Member of the Technical Staff at the Central Research Laboratories of Texas Instruments.

Michael A. Kinch, photograph and biography not available at the time of publication.

Andrew Huntington received the B.S. degree in chemistry from the California Institute of Technology, Pasadena, in 1997. He is currently a graduate student in the Materials Department of the University of California at Santa Barbara.

He specializes in growth of arsenide compounds lattice-matched to InP for optoelectronic applications, including long wavelength multiple-active region vertical-cavity lasers and avalanche photodiodes.

Larry A. Coldren (S'67–M'72–SM'77–F'82) received the Ph.D. degree in electrical engineering from Stanford University, Stanford, CA, in 1972.

After 13 years in the research area at Bell Laboratories, he was appointed Professor of Electrical and Computer Engineering at the University of California at Santa Barbara (UCSB) campus in 1984. In 1986, he assumed a joint appointment with Materials and ECE, and in 2000 the Fred Kavli Chair in Optoelectronics and Sensors. He is also Chairman and Chief Technology Officer of Agility Communications, Inc. At UCSB, his efforts have included work on novel guided-wave and vertical-cavity modulators and lasers as well as the underlying materials growth and fabrication technology. He is now investigating the integration of various optoelectronic devices, including optical amplifiers and modulators, tunable lasers, wavelength-converters, and surface-emitting lasers. He has authored or coauthored over 500 papers, five book chapters, one textbook, and has been issued 32 patents.

Prof. Coldren is a Fellow of the Optical Society of America (OSA) and a past Vice-President of IEEE Laser and Electro-Optics Society (LEOS).

Jean Decobert was born in Lille, France, in 1964. He received the Ph.D. degree in microelectronics from Lille I University in 1993.

Since 1987, he has been working on semiconductor compounds epitaxial growth by MOVPE. He started working on the design of MOVPE reactors and he is particularly involved in aluminum containing semiconductor material for opto- and micro-electronic devices. He joined the National Center of Telecommunication Research (CNET) France Telecom, Bagneux, France, in 1993, where his research focused on the MOVPE growth and fabrication of InP based HEMT and PIN-HEMT devices for OEICs. In 1998, he joined Opto+, Marcoussis, France, the research laboratory founded by Alcatel and France Telecom. Since 2001, he has worked at Alcatel Research and Innovation, Marcoussis, France, where he is in charge of III-V material growth for opto-electronic applications.

Nadine Tscherptner was born in Le Coteau, France, in 1969.

She joined the Alcatel Research and Innovation laboratories, Marcoussis, France, in 1991, in the team of Dr. Eugene Duda where she has developed the process technology of InP devices. Since 2001, she has worked on the MOVPE growth and characterization of III-V semiconductor heterostructures for optoelectronic applications.